

**PARAGENESIS AND COMPOSITION OF BANALSITE, STRONALSITE,  
AND THEIR SOLID SOLUTION IN NEPHELINE SYENITE  
AND ULTRAMAFIC ALKALINE ROCKS**

RUSLAN P. LIFEROVICH<sup>§</sup> AND ROGER H. MITCHELL

*Department of Geology, Lakehead University, 955 Oliver Road, Thunder Bay, Ontario P7B 5E1, Canada*

DMITRIY R. ZOZULYA AND ARKADIY K. SHPACHENKO

*Geological Institute, Kola Science Center, Russian Academy of Science, 14 Fersmana Street, Apatity, 184200, Russia*

ABSTRACT

The paragenesis and compositional variation of banalsite–stronalsite solid-solution series,  $Ba_{1-x}Sr_xNa_2Al_4Si_4O_{16}$ , from five new occurrences in nepheline syenite and ultramafic alkaline rocks are characterized; we also present new data for banalsite and stronalsite from the Benallt mine, in Wales, UK, Långban, in Sweden, and Khibina, in the Kola Peninsula, Russia. Commonly, members of the banalsite–stronalsite solid-solution series occur at the periphery of nepheline crystals in contact with late analcime or albite, and form zoned aggregates grading from banalsite in the cores to barian stronalsite and stronalsite at the margins. Textural relationships show that banalsite might form at a late-magmatic stage, together with nepheline, whereas stronalsite preferentially forms as a byproduct of the postmagmatic conversion of nepheline to analcime, replacing both nepheline and banalsite. This process is facilitated by the similarity of the crystal structures of nepheline and these  $Ba_{1-x}Sr_xNa_2Al_4Si_4O_{16}$  tectosilicates, both of which are based on infinite Si–Al ordered frameworks consisting of –UDUD– rings. The complete  $Ba_{1-x}Sr_xNa_2Al_4Si_4O_{16}$  solid solution and very limited solid solution with lisetite,  $CaNa_2Al_4Si_4O_{16}$ , result from the topological similarity of the structures of banalsite and stronalsite, and significant differences with that of lisetite with respect to cation order.

*Keywords:* stronalsite, banalsite, nepheline, syenite, ijolite, alteration, Prairie Lake, Pilansberg, Sakharjok, Greymakha–Vyrmes, Turiy Mys, Långban.

SOMMAIRE

La paragenèse et la variation en composition de la solution solide banalsite–stronalsite,  $Ba_{1-x}Sr_xNa_2Al_4Si_4O_{16}$ , provenant de cinq nouveaux indices dans la syénite néphélinique ou des roches ultramafiques alcalines, ont fait l'objet d'une description. Nous présentons aussi de nouvelles données pour la banalsite et la stronalsite de la mine Benallt, au Pays de Galles, Långban, en Suède, et à Khibina, dans la péninsule de Kola, en Russie. En général, les membres de la solution solide entre banalsite et stronalsite décorent la bordure de grains de néphéline en contact avec l'analcime tardive ou l'albite, et se présentent en agrégats allant de banalsite dans le noyau à stronalsite barifère et stronalsite à la bordure. Les relations texturales montrent que la banalsite pourrait se former à un stade magmatique tardif, avec la néphéline, tandis que la stronalsite cristallise en général comme sous-produit de la conversion postmagmatique de la néphéline à l'analcime, en remplacement à la fois de néphéline et banalsite. Cette conversion est facilitée par la ressemblance structurale de la néphéline et de ces tectosilicates  $Ba_{1-x}Sr_xNa_2Al_4Si_4O_{16}$ , les deux possédant une trame infinie à Si–Al ordonnés faite d'anneaux –UDUD–. Le fait que la série  $Ba_{1-x}Sr_xNa_2Al_4Si_4O_{16}$  est complète et la solution solide très limitée vers la lisetite,  $CaNa_2Al_4Si_4O_{16}$ , résultent de la ressemblance topologique de la banalsite et la stronalsite, et des différences importantes avec la lisetite par rapport au degré d'ordre des cations.

(Traduit par la Rédaction)

*Mots-clés:* stronalsite, banalsite, néphéline, syénite, ijolite, altération, lac Prairie, Pilansberg, Sakharjok, Greymakha–Vyrmes, Turiy Mys, Långban.

<sup>§</sup> E-mail address: rlife@lakeheadu.ca

## INTRODUCTION

Tectosilicates with the stoichiometry  $ANa_2Al_4Si_4O_{16}$ , where *A* represents Ca, Ba, and Sr, consist of lisetite, banalsite, and stronalsite, respectively. Banalsite and stronalsite are rare minerals that have been described from altered ultramafic xenoliths in alkaline rocks (nepheline syenite, jacupirangite), alkaline ultramafic rocks (nepheline melilitolite), rodingite and jadeitite, and from metasomatic rocks enriched in Fe–Mn oxides and carbonates (Campbell Smith 1944, Welin 1968, Matsubara 1985, Harlow & Olds 1987, Hori *et al.* 1987, Khomyakov *et al.* 1990, Khomyakov 1995, Dunworth & Bell 2003). The “complete solid-solution”  $(Ba_{1-x}Sr_x)Na_2Al_4Si_4O_{16}$  was initially described by Koneva (1996) from the Zhidoy massif, Eastern Sayan, Siberia, Russia, as a minor phase in feldspar–zeolite veins cutting alkaline pyroxenites at the contact with nepheline syenite. The description was based on only three compositions normalized to 100 wt.%.

In this work, we describe five new occurrences of the stronalsite–banalsite solid-solution series (hereafter banalsite–stronalsite<sub>ss</sub>), in nepheline syenite and alkaline ultramafic rocks: the Prairie Lake complex of alkaline rocks and carbonatites, Superior Alkaline Province, northwestern Ontario, Canada, the Pilansberg peralkaline complex, South Africa, the Sakharjok alkaline complex in the Kola Alkaline Province, northwestern Russia, rocks of the peralkaline series in the Gremyakh–Vyrmes complex, and the Turiy Mys complex of ultramafic–alkaline rocks and carbonatites, both also in the Kola Alkaline Province. New compositional data are also presented here for banalsite and stronalsite from previously known occurrences that were used for single-crystal determinations of their structure by Liferovich *et al.* (2006). For this study, we investigated 78 samples of diverse alkaline, alkaline–ultramafic rocks and alkaline metasomatic rocks containing banalsite and stronalsite from nine localities worldwide, and obtained 148 original compositions of these Ba–Sr tectosilicates. These data confirm the existence of a complete solid-solution series between stronalsite and banalsite. A model for the genesis of these minerals is developed on the basis of their textural relationships with other tectosilicates.

## BACKGROUND INFORMATION

The  $(Ba_{1-x}Sr_x)Na_2Al_4Si_4O_{16}$  series adopts space group *Iba2* (Liferovich *et al.* 2006) in contrast to the calcium-dominant analogue, lisetite, which crystallizes in space group *Pbc2<sub>1</sub>* [a non-standard setting of *Pca2<sub>1</sub>* (Rossi *et al.* 1986)]. Both Si and Al are fully ordered in the tetrahedral positions of the framework in both *Iba2*- and *Pbc2<sub>1</sub>*-structured tectosilicates, driving the Si-to-Al ratio to unity according to the aluminum avoidance principle (Loewenstein 1954). These frameworks are topologically similar; they are built up of four-

fold and eight-fold rings consisting of vertex-sharing Si(1)–Al(1) and Si(2)–Al(2) tetrahedra that point alternately up (U) and down (D), thus resulting in a –UDUD– sequence. The structures differ in the location of the large intraframework cations. In lisetite,  $^{VI}Ca$  and  $^{VI}Na$  cations are distributed throughout common Ca + 2Na layers (Rossi *et al.* 1986), whereas in banalsite and stronalsite, the  $^XBa$  or  $^XSr$  and  $^{VI}Na$  cations are ordered, and populate alternate layers parallel to (001), separated by  $\frac{1}{4}c$  (Liferovich *et al.* 2006). This difference precludes the formation of solid solution between banalsite–stronalsite and lisetite (Rossi *et al.* 1986), and presents a structural barrier for the entry of Ca. Structural differences between banalsite–stronalsite and K-feldspar are greater, as the structure of the latter is based on a –UDD– framework (*e.g.*, Deer *et al.* 2001), thus precluding a solid solution between alkali feldspars and Na–Ba–Sr tectosilicates.

Existing compositional data for stronalsite and banalsite are limited and, in some instances, these minerals have been identified only by powder X-ray diffractometry, *e.g.*, banalsite from Långban, Värmland, Filipstad, Sweden (Welin 1968). Some of these data are based on the analysis of bulk samples and thus include other phases. Hence, minor components such as Mg and H<sub>2</sub>O, described for holotype banalsite (Campbell Smith 1944, Campbell Smith *et al.* 1944a, b) undoubtedly result from the presence of impurities. Some data obtained by electron-microprobe analysis do not match the stoichiometry  $ANa_2Al_4Si_4O_{16}$  as a consequence of overestimation of Na, *e.g.*, 2.18–2.38 *apfu* Na in stronalsite (Matsubara 1985, Khomyakov *et al.* 1990, Koneva 1996). Other problems include a significant deficiency of Si at the tetrahedral sites (Matsubara 1985), and analytical discrepancies of up to 2.3 wt.% (Harlow & Olds 1987, Khomyakov *et al.* 1990), which can be hidden in data recalculated to 100 wt.% (Koneva 1996). Significant deviations of the Si-to-Al ratio from unity, *e.g.*, Campbell Smith (1944) and Khomyakov *et al.* (1990), are not in accord with recent single-crystal structural data for banalsite and stronalsite (Liferovich *et al.* 2006).

## ANALYTICAL METHODS

The compositions of stronalsite and banalsite from the localities selected (Table 1) were determined at Lakehead University by energy-dispersion X-ray spectrometry (EDXA) using a JEOL JSM–5900 scanning electron microscope (SEM) equipped with a Link ISIS 300 analytical system incorporating a Super ATW Element Detector (133 eV FWHM MnK). Raw EDXA spectra were acquired with an accelerating voltage of 20 kV, and beam current of 0.475 nA on a Ni standard. The spectra were processed with the LINK ISIS–SEMQUANT quantitative software package, with full ZAF corrections applied. The following well-characterized standards were used: jadeite (Na), wollastonite

TABLE 1. OCCURRENCES OF STRONALSITE, BANALSITE AND THE STRONALSITE–BANALSITE SOLID-SOLUTION SERIES IN ALKALINE ROCKS

| Occurrence                                    | Description                         | Host rock  | Paragenesis   |
|---|-------------------------------------|--|---|
| Turiy Mys, <sup>1</sup><br>Kola, Russia       | Stronalsite, end-member             | Nepheline melilitolite                                   | Ne, Mel, mica, Cal, Prv, Mgt  |
|   | Banalsite, end-member               | Melteigite, ijolite                                      | Ne, Adr, Cpx, FAp, Ilm, Anl, Pct, Cal   |
|   | Banalsite-stronalsite <sub>ss</sub> | Ijolite  | Ne, Adr, Cpx, FAp, Ilm, Anl, Pct, Cal   |
| Khibina, <sup>2,3</sup><br>Kola, Russia       | Stronalsite, end-member             | Hydrothermally altered<br>Mel–Cus xenoliths <sup>2</sup> | Ne, Adr, Mel, REE-rich FAp, Bth,<br>barian manganoan Bt, Str, Cpx, Cal, Wo,<br>Czr, Cus, Mgt, Glc, Mn-rich Pct, Mn-rich Ilm |
| Långban, Sweden                               | Banalsite, end-member               | Alkaline glimmerite                                      | Phl, Cpx, Mpb, Mac, Roe, Brt, Ntr and other zeolites, Cal   |
| Pilansberg,<br>South Africa                   | Banalsite, end-member               | Lujavrite,   | Ne, Anl, Lct, (Ecn–Pyf) <sub>ss</sub> , Zrn, Str, deuteric Na–Zr-   |
|   | Banalsite-stronalsite <sub>ss</sub> | foyaite,   | silicate(s), Bt, Aln, Anc, microphases of Sr, REE, Zr, and  |
|   | Stronalsite, end-member             | "Ledig" foyaite  | Nb, Sap, Fl, Clb  |
| Prairie Lake,<br>Ontario, Canada              | Stronalsite, end-member             | Melteigite, ijolite,                                     | Ne replaced by Anl and Ntr, Ca–Na zeolites; Prc, Rt, Adr,   |
|   | Banalsite-stronalsite <sub>ss</sub> | glimmerite,<br>clinopyroxenite                           | Srm, Zr-rich Ttn, Hlp, Pcl (?), Slw, Fap, Btc, Lop–(Ce), Mrl,<br>sulfides   |
| Gremyakh–Vyrmes,<br>Kola Peninsula,<br>Russia | Banalsite-stronalsite <sub>ss</sub> | Urtite   | Ne replaced by Anl + Ab + white mica; Py, Fap, Zr–Fe–Al-<br>bearing Ttn, Bt, Cal, Ilm, Mgt, Fpr, Ba-bearing Kfs             |
| Sakharjok, Kola<br>Peninsula, Russia          | Banalsite-stronalsite <sub>ss</sub> | Essexite   | Ne, Cpx, Phl, Ed, Ab, Cbt–Gdf, Fap, Nc, Prc, Y-rich Bth   |
| Zhidoy, East Sayan,<br>Russia <sup>4</sup>    | Banalsite-stronalsite <sub>ss</sub> | Late veinlets cutting<br>alkaline pyroxenite             | Anl, Ntr, Ccn, Ank, Prh, Brt  |

Symbols: Ab: albite, Aln: allanite, Anl: analcime, Anc: ancylite-(Ce), Adr: andradite, Ank: ankerite, Brt: barite, Bt: biotite, Btc: barytocalcite, Bth: britholite, Cal: calcite, Ccn: cancrinite, Cbt: cobaltite, Cpx: clinopyroxene, Cus: cuspidine, Czr: calzirtite, Ecn: ecandrewsite, Ed: edenite, Fap: fluorapatite, Fl: fluorite, Fpr: ferropargasite, Gdf: gersdorffite, Glc: glaucocroite, Hlp: hyalophane, Ilm: ilmenite, Lct: leucite, Lop–(Ce): loparite-(Ce), Mac: macedonite, Mgt: magnetite, Mpb: magnetoplumbite, Mel: melilite, Ntr: natrolite, Ne: nepheline, Pct: pectolite, Prh: prehnite, Prv: perovskite, Phl: phlogopite, Py: pyrite, Prc: pyrochlore, Pyf: pyrophanite, Roe: roebingite, Rt: rutile, Sap: strontium-apatite, Srm: schorlomite, Slw: slawsonite, Str: strontianite, Ttn: titanite, Wo: wollastonite, Zrn: zircon. References: 1 Dunworth & Bell (2003), 2 Khomyakov *et al.* (1990), 3 Koneva (1996), Liferovich *et al.* (2006).

(Ca), orthoclase (K), corundum (Al), pyroxene glass DJ35 (Si), barite (Ba), ilmenite (Fe), and SrTiO<sub>3</sub> (Sr).

To reduce analytical errors due to the possible loss of Na resulting from electron-beam-induced damage, raster scanning and reduced periods of counting of 50 s (live time) were employed. Reproducibility within the analytical errors of the compositions of stronalsite and banalsite, and the agreement of the cation proportions obtained for all samples with the theoretical stoichiometry of stronalsite and banalsite, demonstrate the reliability of these data. The accuracy of the EDXA method was cross-checked by analysis of sodic silicate and oxide minerals by wavelength-dispersion electron-microprobe analysis (WDS–EMPA) using an automated CAMECA SX–50 electron microprobe (University of Manitoba) following methods described by Mitchell & Vladykin (1993) and Chakhmouradian & Mitchell

(1999, 2002). In addition, the accuracy of the analytical results on stronalsite and banalsite was verified every 1–1.5 hours using natural lueshite, perovskite, loparite, eudialyte, benitoite, villiaumite, and jadeite, previously analyzed in several laboratories by WDS–EMPA. High-resolution back-scattered electron (BSE) imagery was used to confirm the absence of small inclusions of any foreign Na-, Sr- and Ba-bearing phases.

The majority of stronalsite and banalsite compositions obtained in this study can be satisfactory recalculated to the general formula (Ba,Sr)Na<sub>2</sub>Al<sub>4</sub>Si<sub>4</sub>O<sub>16</sub>. Relatively few samples, mostly from rocks subjected to epithermal alteration and weathering, show deviation from this “ideal” stoichiometry resulting from leaching of the large cations, Na, Ba, and Sr. The nature and intensity of alteration processes differ from rock to rock, and vary from massif to massif. Varying degrees

of cation loss no doubt result from the differing compositions of postmagmatic fluids and  $P$ - $T$  parameters of the alteration processes. Discussion of the alteration of banalsite–stronalsite<sub>ss</sub> is beyond the scope of the present work.

As structural factors preclude occupancy of cations other than Na, Sr and Ba at the <sup>VI</sup>Na and <sup>X</sup>A sites in the structures of stronalsite and banalsite (see above), the compositional variation of the unaltered banalsite–stronalsite<sub>ss</sub> can be characterized in terms of only two end-members, or simply in terms of the <sup>X</sup>A-site occupancy by Ba versus Sr.

#### BANALSITE AND STRONALSITE FROM PREVIOUSLY DESCRIBED OCCURRENCES: NEW DATA

##### Banalsite

Banalsite from Långban (Värmland, Filipstad, Sweden) was first identified by X-ray powder-diffraction methods by Welin (1968). The mineral occurs in a medium- to fine-grained alkaline glimmerite, consisting of Ba-bearing phlogopite (1.8–2.2 wt.% BaO), prismatic clinopyroxene (aegirine–hedenbergite), abundant natrolite, an unidentified Ca–Na zeolite(s), and minor calcite (Fig. 1a, Table 1). Banalsite is associated with diverse rare Pb–Mn–Fe oxides and oxy salt species, including

magnetoplumbite, macedonite, and roeblingite (Welin 1968). Banalsite is enclosed by natrolite and Na–Ca zeolite(s) and has been subjected to deuteric alteration at the contact with these silicates. The alteration results in the corrosion and formation of numerous small inclusions of barite at the periphery of the banalsite grains. Fresh banalsite has an end-member composition (Table 2, comp. 1, 2; Fig. 2), with low to undetectable Sr, K, and Ca. The Si-to-Al ratio is very close to unity. These compositional data agree well with site occupancies obtained by a single-crystal determination of the structure undertaken on the same material (Liferovich *et al.* 2006).

At the Benallt mine (Rhiw Peninsula, Wales, UK), banalsite occurs in late-forming veinlets cutting metamorphosed Mn–Fe carbonate ores. The mineral is associated with calcite, natrolite, tephroite, jacobsonite, alleghanyite, pyrophanite, Mn-rich biotite, andradite, harmotome, and apatite (Campbell Smith 1944, Campbell Smith *et al.* 1944a, b). In places, aggregates of euhedral grains of banalsite (1–5 mm) form up to 80 vol.% of the veinlets, and are intergrown with celsian (or paracelsian?) and barite (Fig. 1b). In contrast to the bulk wet-chemistry data available (Campbell Smith 1944, Campbell Smith *et al.* 1944a, b), our data indicate that the mineral conforms to the banalsite end-member composition (Fig. 2), with no significant analytical discrepancies or detectable Mg and K (Table 2, comp. 3, 4).

##### Stronalsite

Stronalsite from the Khibina peralkaline complex in the Kola Alkaline Province was first recognized in a drill-core sample by Khomyakov *et al.* (1990). The mineral forms botryoidal aggregates of small co-oriented grains enclosed by an unusual Na–Sr-rich variety of melillite. Previously published data (Khomyakov *et al.* 1990, Khomyakov 1995) on the composition of stronalsite from this locality are considered to be unreliable, as Na is overestimated and Ba + Sr ( $\pm$ Ca) are underestimated. In addition, there are significant deviations of the Si-to-Al ratio from unity. These data are at variance with the structural data of Liferovich *et al.* (2006) for this sample of stronalsite. Our further study of the drill-core material resulted in the recognition of a sample containing homogeneous crystals of stronalsite measuring up to 4 mm in size in a strongly altered xenolith of cuspidine–melilite rock hosted by nepheline syenite. A detailed petrographic description of similar xenoliths and their alteration is given by Khomyakov *et al.* (1990). Our data show that stronalsite from Khibina has an end-member composition (Fig. 2), and the Ba content does not exceed ~0.2 wt.% BaO. The mineral contains up to 0.8 wt.% Fe<sub>2</sub>O<sub>3</sub> with no detectable Ca (Table 2, comp. 5, 6). On the basis of textural relationships, stronalsite is interpreted to be a

TABLE 2. COMPOSITIONS OF BANALSITE AND STRONALSITE FROM DIVERSE LOCALITIES

| e.s.d.                           | Långban |        | Wales  |        | Khibina |        | Prairie Lake |        |        |
|----------------------------------|---------|--------|--------|--------|---------|--------|--------------|--------|--------|
|                                  | 1       | 2      | 3      | 4      | 5       | 6      | 7            | 8      |        |
| SiO <sub>2</sub> wt.%            | 0.19    | 36.21  | 35.61  | 36.43  | 36.71   | 40.33  | 38.89        | 39.28  | 39.78  |
| Al <sub>2</sub> O <sub>3</sub>   | 0.17    | 31.05  | 31.32  | 31.03  | 30.35   | 34.74  | 34.09        | 33.29  | 33.51  |
| Fe <sub>2</sub> O <sub>3</sub> * | 0.15    | -      | -      | -      | -       | 0.81   | 1.02         | 1.02   | 0.94   |
| CaO                              | 0.05    | -      | -      | 0.14   | -       | -      | -            | 0.42   | 0.18   |
| SrO                              | 0.28    | -      | 0.54   | -      | -       | 15.90  | 16.01        | 14.48  | 15.19  |
| BaO                              | 0.24    | 23.45  | 22.89  | 22.90  | 22.79   | 0.21   | -            | 0.36   | 0.62   |
| Na <sub>2</sub> O                | 0.15    | 9.36   | 9.38   | 9.40   | 9.49    | 10.40  | 10.05        | 10.16  | 9.97   |
| K <sub>2</sub> O                 | 0.05    | -      | -      | -      | -       | -      | -            | 0.26   | 0.33   |
| Total                            |         | 100.07 | 99.74  | 99.90  | 99.34   | 101.58 | 99.85        | 99.27  | 100.52 |
| Si <i>apfu</i>                   | 0.001   | 3.980  | 3.930  | 3.994  | 4.045   | 3.997  | 3.939        | 3.989  | 4.003  |
| Al                               | 0.013   | 4.022  | 4.074  | 4.009  | 3.941   | 4.057  | 4.069        | 3.984  | 3.975  |
| Fe                               | 0.007   | -      | -      | -      | -       | -      | 0.062        | 0.078  | 0.072  |
| Si:Al                            |         | 0.989  | 0.965  | 1.00   | 1.03    | 0.985  | 0.968        | 1.001  | 1.007  |
| Ca                               | 0.005   | -      | -      | 0.016  | -       | -      | -            | 0.046  | 0.019  |
| Sr                               | 0.016   | -      | 0.035  | -      | -       | 0.914  | 0.940        | 0.853  | 0.886  |
| Ba                               | 0.009   | 1.010  | 0.990  | 0.984  | 0.984   | 0.008  | -            | 0.014  | 0.024  |
| ΣA                               |         | 1.010  | 1.025  | 1.000  | 0.984   | 0.922  | 0.940        | 0.913  | 0.929  |
| Sr:Ba                            |         | -      | 0.035  | -      | -       | 114.25 | -            | 59.52  | 36.26  |
| Na                               | 0.028   | 1.995  | 2.007  | 1.998  | 2.027   | 1.998  | 1.973        | 2.000  | 1.945  |
| K                                | 0.007   | -      | -      | -      | -       | -      | -            | 0.034  | 0.042  |
| Σcations                         |         | 11.006 | 11.036 | 11.001 | 10.998  | 10.974 | 10.982       | 10.997 | 10.967 |

e.s.d.: estimated standard deviation ( $\sigma$ ); \* total iron is given as Fe<sub>2</sub>O<sub>3</sub>; - not detected. The structural formulae are calculated on the basis of 16 atoms of oxygen.

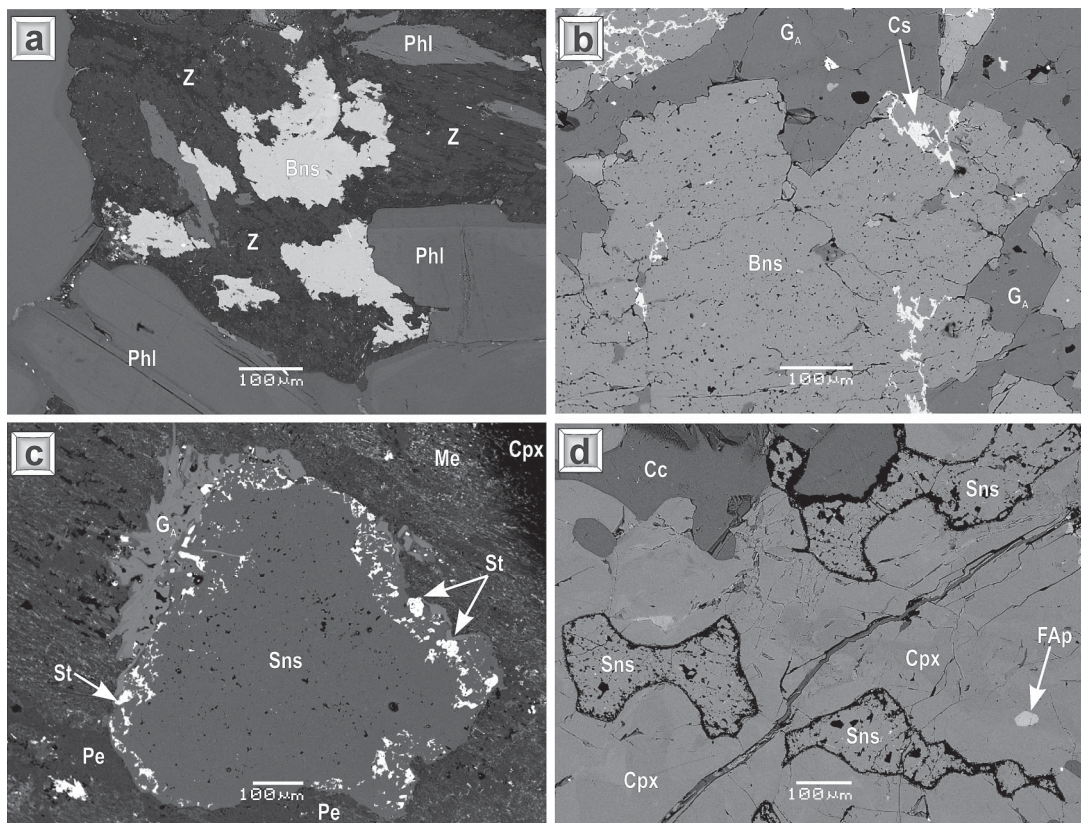


FIG. 1. Back-scattered-electron images (BSE) of stronalsite and banalsite. a. Banalsite in an alkaline glimmerite, Långban, Filipstad, Värmland, Sweden. b. Banalsite in manganese carbonate ores, Benallt mine, Rhiw Peninsula, Wales, UK. c. Stronalsite in an altered xenolith of cuspidine–melilite rock, Khibina peralkaline complex, Kola Alkaline Province, Russia. d. Stronalsite in a xenolith of alkaline clinopyroxenite, Prairie Lake alkaline complex, northwestern Ontario, Canada. Here, and in other BSE images: Ab: albite, Anl: analcime, Bns: banalsite, BS<sub>ss</sub>: banalsite–stronalsite solid-solution series, Cc: calcite, Cpx: clinopyroxene, FAP: fluorapatite, G<sub>A</sub>: andradite, G<sub>S</sub>: schorlomite, Me: strontian melilite, Ne: nepheline, Pe: manganian pectolite, Phl: phlogopite, Sns: stronalsite, Sod: sodalite, St: strontianite, Z: zeolite (or a mixture of unidentified zeolites).

metasomatic phase formed by a relatively high-temperature alteration of Na–Sr-rich melilite and nepheline. The stronalsite, in turn, was commonly subjected to further low-temperature alteration, with formation of abundant inclusions of strontianite within altered marginal areas (Fig. 1c). Unaltered stronalsite is preserved only where it is mantled by more stable silicates, *e.g.*, andradite (Fig. 1c). The occurrence of stronalsite in the cuspidine–melilite rock at Khibina might be similar to that described from cuspidine-bearing nepheline melilitolite at the Turiy Mys ultramafic–alkaline complex, Kola Alkaline Province, Russia (Dunworth & Bell 2003).

#### NEW OCCURRENCES OF BANALSITE–STRONALSITE SOLID-SOLUTION SERIES IN NEPHELINE SYENITE AND ALKALINE ULTRAMAFIC ROCKS

*The Sakharjok alkaline massif,  
Kola Alkaline Province*

At Sakharjok, the banalsite–stronalsite solid-solution series was identified in a medium-grained essexite. Large xenoliths of this rock occur in trachtyoid nepheline syenite, and the sample containing banalsite–stronalsite<sub>ss</sub> represents the contact zone with the feldspathoidal host-rock. The geological setting and textural characteristics of the essexite are given by Batieva & Belkov (1984) and Zozulya *et al.* (2001). The rock consists of flow-aligned prismatic titanian aegirine-

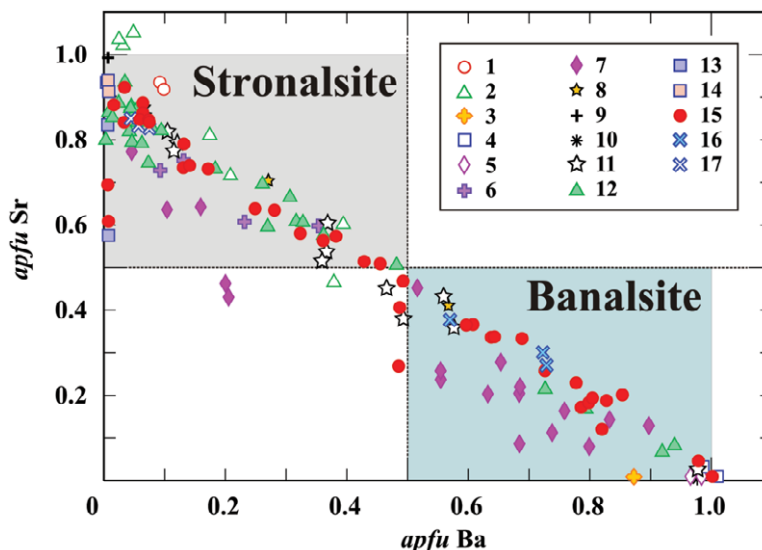


FIG. 2. Compositional variation of banalsite, stronalsite, and banalsite–stronalsite solid-solution. Occurrences 1–5 are related to metamorphic and metasomatic rocks: 1: in altered mafic metatuff, Rendai, Kochi City, Japan [stronalsite holotype (Hori *et al.* 1987)], 2: in jadeite–serpentine rock, Ohsa, Okayama, Japan (Hori *et al.* 1987), 3: in jadeitites, Burma (Harlow & Olds 1987), 4: in alkaline glimmerite, Långban, Värmland, Filipstad, Sweden, 5: in late veins cutting manganiferous mudstone, Benallt mine, Wales, UK (banalsite holotype); 6–7: occurrences related to “miaskitic” nepheline syenite complexes; 6: in essexite, Sakharjok, Kola Alkaline Province, Russia, 7: in urtite, Gremyakha–Vyrmes, Kola Alkaline Province, Russia; 8–12: occurrences related to alkaline–ultramafic complexes with carbonatites; 8: in late feldspar–zeolite veins cutting alkaline pyroxenite, Zhidoy complex, East Sayan, Russia (Koneva 1996), 9: in melilitolite and 10: in melteigite, Turiy Mys complex, Kola Alkaline Province, Russia (Dunworth & Bell 2003), 11: in ijolite, Turiy Mys complex, Kola Alkaline Province, Russia, 12: in ijolite, wollastonite ijolite and in clinopyroxenite xenoliths, Prairie Lake Complex, Ontario, Canada; 13–17: occurrences related to sodic peralkaline nepheline syenite complexes; 13: in altered cuspidine–melilite xenolith Khibina, Kola Alkaline Province, Russia (Khomyakov *et al.* 1990), 14: the same occurrence, as described in this work, 15: in lujavrite, 16: in foyaite, and 17: in “Ledig” foyaite, Pilansberg complex, South Africa.

augite, phlogopite, nepheline, microcline, analcime, and plagioclase (An<sub>20–30</sub>). Cancrinite and natrolite are post-magmatic phases. Accessories present include zircon, titanian magnetite, pyrochlore, fluorite, meliphanite, Y-rich britholite, nickeline, and cobaltite–gersdorffite. Nepheline shows incipient replacement by analcime and natrolite (Figs. 3a, b), and has the composition Ne<sub>88</sub>Ks<sub>10</sub>Qtz<sub>02</sub> (average of three analyses), and contains 1.5–1.8 wt.% Fe<sub>2</sub>O<sub>3</sub>. This Na-enriched composition does not fall into the Morozewicz–Burger convergence field and is similar to the most sodic nepheline reported from augite syenite at Ilímaussaq (Markl *et al.* 2001). These low-Si compositions may originate by recrystallization at temperatures below 500°C (Hamilton 1961, Wilkinson & Hensel 1994). Banalsite–stronalsite<sub>ss</sub> occurs as aggregates of small co-oriented grains ( $\leq 5 \mu\text{m}$ ). These aggregates are confined to the periphery of nepheline crystals, adjacent to clinopyroxene and analcime (Fig. 3b). The series is preferentially enriched in Sr (Fig. 2), and varies in composition from barian stronalsite in the core of the aggregates to stronalsite at

their margins. The banalsite–stronalsite<sub>ss</sub> contains low but detectable Ca (0.3–0.6 wt.% CaO) and no detectable K (Table 3, comp. 1–4).

#### *The Gremyakha–Vyrmes complex, Kola Alkaline Province*

The banalsite–stronalsite series is found in massive coarse-grained urtite from the Gremyakha–Vyrmes complex of mafic–ultramafic rocks, quartz syenites and feldspathoidal rocks. Sr–Nd isotope data (Arzamastsev *et al.* 2003) show that the latter series of rocks was derived from a specific mantle-source and is not comagmatic with other rocks of the Gremyakha–Vyrmes complex. The feldspathoidal rocks, emplaced in layered peridotite–gabbro–anorthosite–monzogabbro series, vary from urtite and ijolite to jacupirangite in mode and appear as a series of spatially close stocks, each measuring a few tens of meters in diameter. Aggregates of white mica (“sericite”), zeolites and oxides of Fe and Al commonly replace nepheline. Massive

coarse-grained urtite consists of 70–75 vol.% nepheline with subordinate amounts of aegirine-augite and ferropargasite. Minor and accessory phases in this rock are K-feldspar, titanite, calcite, pyrite, fluorapatite, barium biotite, Ba-bearing K-feldspar, ilmenite and magnetite. Nepheline is impregnated with abundant microlites of clinopyroxene and exhibits a stoichiometric composition falling in the Morozewicz–Burger convergence field. The mode of nepheline alteration in urtite differs from that in other feldspathoidal rocks in the Gremyakha–Vyrmes complex by the absence of white mica and oxides of Fe and Al. In contrast, this nepheline has been subjected to corrosion, with partial replacement by albite, natrolite, and unidentified Na–Ca zeolite(s). Banalsite–stronalsite<sub>ss</sub> occurs only in white-mica-free urtite, and forms as aggregates of small co-oriented grains that mantle and replace nepheline at the contact with albite and zeolites (Fig. 3c). In places, nepheline is completely replaced by zeolites, which also contain aggregates of banalsite–stronalsite<sub>ss</sub> (Fig. 3d). The composition of the banalsite–stronalsite series (Table 3, comp. 5–8) varies from 90 to 5 mol.% of the banalsite end-member (Fig. 2). Up to 0.15 *apfu* Ca (~1.4

wt.% CaO) is observed in the cation-deficient <sup>X</sup>A site. We consider that this value is the empirical limit of entry of calcium in the banalsite–stronalsite solid solution, as this is the most Ca-rich composition encountered in this work. The <sup>V</sup>Na site in the banalsite–stronalsite series is completely filled by Na.

*Turiy Mys ultramafic–alkaline complex,  
Kola Alkaline Province*

The geology and mineralogy of the Turiy Mys ultramafic–alkaline complex and associated carbonatites were described by Kukharenco *et al.* (1965), Bell *et al.* (1996), and Dunworth & Bell (2003). In addition to stronalsite and banalsite observed in melilitolite and nepheline syenite, respectively (Dunworth & Bell 2003), our study demonstrates the presence of members of the banalsite–stronalsite series in late leucocratic ijolite, which encloses the main phoscorite–carbonatite stock in the central part of the complex. The banalsite–stronalsite series is recognized as a late-forming phase in drill-core samples of ijolite that are cut by veins of coarse-grained calciocarbonatite and fine-

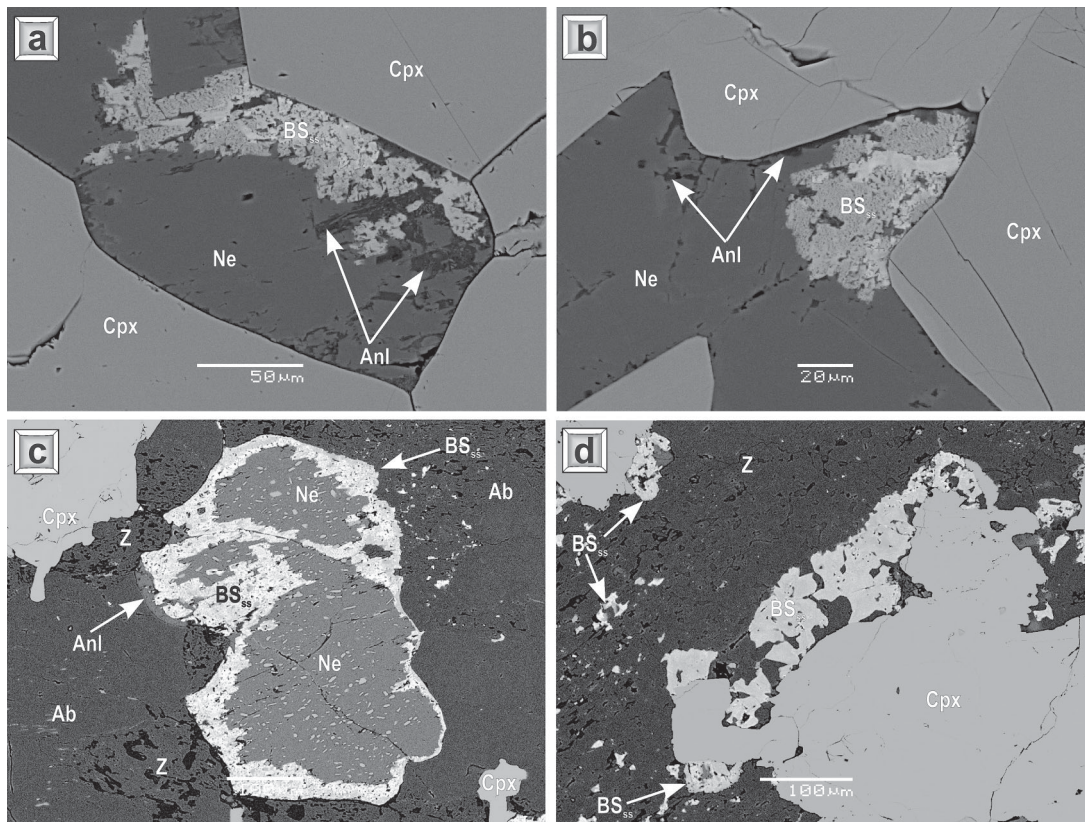


FIG. 3. Back-scattered-electron images showing textural features of the banalsite–stronalsite solid-solution; a, b: in essexite, Sakharjok and c, d: in urtite, Gremyakha–Vyrmes, Kola Alkaline Province, Russia.

grained banded phoscorite. The rock was subjected to alteration which, most probably, was associated with emplacement of the fluid-rich carbonatitic magma. The alteration resulted in replacement (mantling) of primary phlogopite, diopside, andradite and nepheline by tetra-ferriphlogopite, aegirine, schorlomite and analcime, respectively. Minor and accessory phases present are sodalite, cancrinite, fluorapatite (1.2–1.8 wt.% SrO), barytolamprophyllite, manganoan ilmenite, titanian magnetite, natrolite, gonnardite(?), pectolite, calcite, burbankite, and sulfides. Relics of corroded and partially replaced crystals of nepheline in this rock have the composition  $\text{Ne}_{77}\text{Ks}_{23}\text{Qtz}_0$ , emphasizing the extensive low-temperature re-equilibration of this mineral. Textural relationships show that the banalsite–stronalsite series was formed by replacement of nepheline at the contact with analcime, the latter being the main product of nepheline breakdown. The banalsite–stronalsite<sub>ss</sub> never forms where nepheline has been replaced by sodalite (*e.g.*, Fig. 4a) or cancrinite. The banalsite–stronalsite<sub>ss</sub> aggregates are zoned and

grade in composition from end-member banalsite to end-member stronalsite (Fig. 2). The observed differences in average atomic number (AZ) on back-scattered electron (BSE) images result primarily from variations in Ba and Sr content (Table 3, comp. 9–12). Banalsite (high-AZ areas on Fig. 4a), the earliest phase, occurs at the immediate contact with nepheline, whereas stronalsite is found at the margins of banalsite–stronalsite aggregates, adjacent to analcime. The amounts of Ca, K, and Fe in banalsite–stronalsite<sub>ss</sub> from Turiy Mys ijolite are negligible.

#### *The Pilansberg peralkaline complex, South Africa*

The Pilansberg complex is one of the largest and mineralogically complex peralkaline massifs in the world. The geology of the complex is as yet inadequately characterized, and only reconnaissance studies have been published by Shand (1928), Retief (1962, 1963), Ferguson (1973), and Lurie (1973, 1986). The only modern mineralogical investigations are

TABLE 3. COMPOSITION OF THE BANALSITE–STRONALSITE SOLID-SOLUTION SERIES IN NEPHELINE SYENITE FROM ALKALINE COMPLEXES OF THE KOLA ALKALINE PROVINCE, NORTHWESTERN RUSSIA

|                                  | Sakharjok |        |        |        | Gremyakh–Vyrmes |        |        |        | Turiy Mys |        |        |        |
|----------------------------------|-----------|--------|--------|--------|-----------------|--------|--------|--------|-----------|--------|--------|--------|
|                                  | 1         | 2      | 3      | 4      | 5               | 6      | 7      | 8      | 9         | 10     | 11     | 12     |
| SiO <sub>2</sub> wt.%            | 38.49     | 40.04  | 39.67  | 40.29  | 37.87           | 37.25  | 40.22  | 40.25  | 37.02     | 37.84  | 39.12  | 38.90  |
| Al <sub>2</sub> O <sub>3</sub>   | 32.71     | 32.93  | 33.40  | 33.05  | 32.14           | 32.80  | 33.28  | 33.62  | 30.55     | 32.66  | 33.74  | 33.92  |
| Fe <sub>2</sub> O <sub>3</sub> * | -         | -      | 0.14   | 0.44   | -               | -      | -      | 0.34   | 0.51      | -      | -      | -      |
| CaO                              | 0.51      | 0.58   | 0.31   | 0.50   | -               | -      | 0.46   | 1.38   | -         | 0.45   | -      | 0.33   |
| SrO                              | 9.91      | 10.29  | 12.72  | 12.40  | 3.33            | 7.37   | 10.97  | 13.35  | 0.14      | 7.41   | 13.85  | 14.83  |
| BaO                              | 8.67      | 5.81   | 3.29   | 2.34   | 16.44           | 12.44  | 4.03   | 1.18   | 22.86     | 11.30  | 2.62   | 1.58   |
| Na <sub>2</sub> O                | 9.50      | 10.26  | 9.56   | 10.05  | 9.96            | 9.72   | 10.70  | 10.59  | 9.35      | 9.85   | 10.13  | 10.19  |
| K <sub>2</sub> O                 | -         | -      | -      | -      | 0.18            | -      | 0.31   | -      | 0.10      | -      | -      | -      |
| Total                            | 99.79     | 99.91  | 99.09  | 99.07  | 99.92           | 99.58  | 99.97  | 100.71 | 100.53    | 99.51  | 99.46  | 99.75  |
| Si ( <i>apfu</i> )               | 4.007     | 4.078  | 4.048  | 4.083  | 4.021           | 3.946  | 4.066  | 4.018  | 4.035     | 3.979  | 3.993  | 3.959  |
| Al                               | 4.013     | 3.953  | 4.016  | 3.947  | 4.022           | 4.095  | 3.965  | 3.956  | 3.925     | 4.047  | 4.059  | 4.069  |
| Fe                               | -         | -      | 0.011  | 0.034  | -               | -      | -      | 0.026  | 0.042     | -      | -      | -      |
| Si:Al                            | 0.998     | 1.032  | 1.008  | 1.034  | 1.000           | 0.964  | 1.025  | 1.016  | 1.028     | 0.983  | 0.984  | 0.973  |
| Ca                               | 0.057     | 0.063  | 0.034  | 0.054  | -               | -      | 0.050  | 0.148  | -         | 0.051  | -      | 0.036  |
| Sr                               | 0.598     | 0.608  | 0.753  | 0.729  | 0.205           | 0.453  | 0.643  | 0.773  | 0.009     | 0.452  | 0.820  | 0.875  |
| Ba                               | 0.354     | 0.232  | 0.132  | 0.093  | 0.684           | 0.516  | 0.160  | 0.046  | 0.976     | 0.466  | 0.105  | 0.063  |
| ΣA                               | 1.009     | 0.903  | 0.919  | 0.876  | 0.889           | 0.969  | 0.853  | 0.967  | 0.985     | 0.969  | 0.925  | 0.974  |
| Sr:Ba                            | 1.691     | 2.621  | 5.721  | 7.842  | 0.300           | 0.877  | 4.028  | 16.742 | 0.009     | 0.970  | 7.823  | 13.890 |
| Na                               | 1.917     | 2.026  | 1.891  | 1.975  | 2.050           | 1.996  | 2.097  | 2.050  | 1.976     | 2.008  | 2.005  | 2.011  |
| K                                | -         | -      | -      | -      | 0.024           | -      | 0.040  | -      | 0.014     | -      | -      | -      |
| Σcations                         | 10.946    | 10.959 | 10.884 | 10.914 | 11.006          | 11.005 | 11.020 | 11.016 | 10.977    | 11.002 | 10.980 | 11.012 |

\* total iron is given as Fe<sub>2</sub>O<sub>3</sub>; - not detected. The structural formulae calculated on the basis of 16 atoms of oxygen.



those of Olivo & Williams-Jones (1999) and Mitchell & Liferovich (2005) on eudialyte, and Mitchell & Liferovich (2004) on the eandrewsite–pyrophanite solid-solution series.

The major nepheline syenite series comprising the Pilansberg complex are lujavrite (trachytoid, inequigranular and porphyroblastic “green foyaite”), foyaite (coarse-grained “white foyaite”), and albite–aegirine rocks enriched in Nb, Zr, Sr, Th, and LREE (light rare-earth elements) termed “Ledig foyaite” (a local name). Current research (Mitchell & Liferovich 2004, 2005) on the mineralogy and petrology of the major nepheline syenite units has demonstrated extensive autometasomatic alteration, which has resulted in the development of complex postmagmatic parageneses grading in alkalinity from miaskitic to hyperagpaitic. Banalsite, stronalsite and members of the solid solution are found throughout the postmagmatic parageneses in all varieties of the feldspathoidal syenite.

The margins of stubby crystals of nepheline in lujavrite have trapped anhedral grains of banalsite

(*e.g.*, Table 4, comp. 3) along discontinuous concentric zones. At the postmagmatic stage, this mineral was gradually converted to botryoidal aggregates of banalsite–stronalsite<sub>ss</sub> (Table 4, comp. 4–12), in parallel with replacement of nepheline by analcime. In common with the other above-described occurrences in nepheline syenite, most of the banalsite–stronalsite<sub>ss</sub> in the Pilansberg syenites was formed at the expense of nepheline. Nepheline in the least-altered Pilansberg nepheline syenite has the composition  $Ne_{72}Ks_{19}Qtz_{09}$  and contains 2.5 wt.%  $Fe_2O_3$ . This composition falls within the Morozewicz–Burger convergence field, and indicates crystallization of nepheline at temperature below 580–600°C (Hamilton 1961, Wilkinson & Hensel 1994). Corroded nepheline partially replaced by analcime and mantled by banalsite–stronalsite<sub>ss</sub> aggregates (Figs. 4b, d) approaches the stoichiometric composition in parallel with removal of Fe, thus suggesting recrystallization in contact with a deuteric fluid phase (Mitchell & Liferovich 2005). In common with the Turiy Mys and Prairie Lake occurrences (see below), the banal-

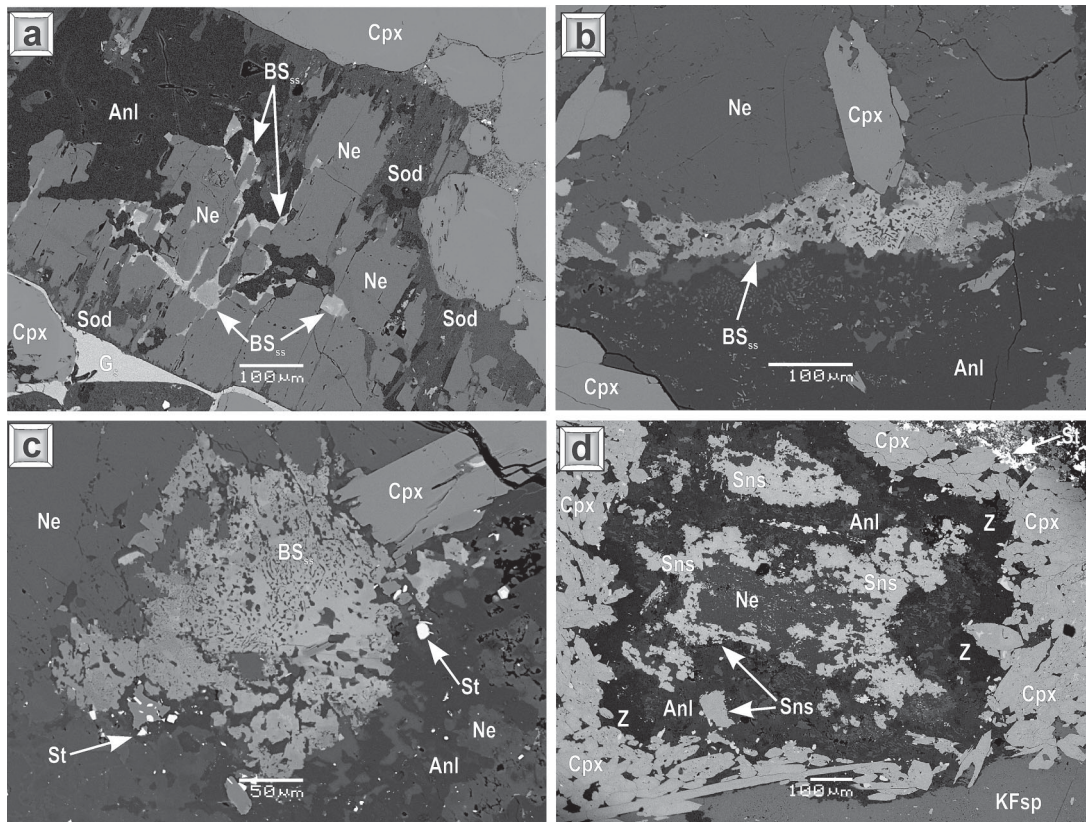


FIG. 4. Back-scattered-electron images showing textural features of the banalsite–stronalsite solid-solution; a: in ijolite, Turiy Mys complex, Kola Alkaline Province, Russia; b, c: in lujavrite and d: in “Ledig” foyaite, Pilansberg peralkaline complex, South Africa.

TABLE 4. COMPOSITION OF THE BANALSITE-STRONALSITE SOLID-SOLUTION SERIES IN NEPHELINE SYENITE FROM THE PILANSBERG PERALKALINE COMPLEX, SOUTH AFRICA, AND IN IJOLITE FROM PRAIRIE LAKE, NORTHWESTERN ONTARIO, CANADA

| wt.%                             | Pilansberg |        |        |        |        |        |        |        |        |        |        | Prairie Lake |        |        |        |        |        |        |        |
|----------------------------------|------------|--------|--------|--------|--------|--------|--------|--------|--------|--------|--------|--------------|--------|--------|--------|--------|--------|--------|--------|
|                                  | 1          | 2      | 3      | 4      | 5      | 6      | 7      | 8      | 9      | 10     | 11     | 12           | 13     | 14     | 15     | 16     | 17     | 18     | 19     |
| SiO <sub>2</sub>                 | 36.92      | 38.03  | 36.49  | 37.66  | 37.42  | 37.43  | 38.65  | 38.44  | 38.83  | 39.13  | 40.08  | 40.33        | 40.03  | 36.54  | 36.77  | 37.81  | 38.80  | 40.21  | 39.29  |
| Al <sub>2</sub> O <sub>3</sub>   | 31.66      | 32.39  | 30.63  | 31.15  | 31.27  | 32.09  | 32.50  | 32.96  | 33.26  | 33.78  | 33.65  | 33.85        | 33.32  | 31.53  | 31.99  | 32.29  | 32.58  | 32.98  | 33.56  |
| Fe <sub>2</sub> O <sub>3</sub> * | -          | -      | 0.33   | -      | -      | -      | -      | -      | -      | -      | 0.27   | -            | 0.31   | 0.36   | 0.66   | 0.36   | 0.24   | 1.32   | 0.36   |
| CaO                              | -          | -      | -      | -      | -      | -      | 0.06   | -      | -      | -      | -      | -            | -      | 0.10   | 0.00   | 0.07   | 0.21   | 0.06   | 0.00   |
| SrO                              | 4.33       | 6.19   | 0.64   | 3.12   | 4.13   | 5.450  | 6.72   | 9.35   | 10.63  | 13.37  | 14.48  | 15.16        | 14.49  | 1.07   | 3.44   | 8.27   | 11.59  | 13.52  | 14.78  |
| BaO                              | 17.24      | 13.84  | 22.77  | 19.10  | 17.19  | 15.27  | 11.91  | 8.86   | 6.96   | 3.30   | 1.87   | 0.42         | 1.13   | 21.63  | 17.24  | 11.65  | 6.44   | 1.59   | 1.11   |
| Na <sub>2</sub> O                | 9.54       | 10.23  | 9.44   | 9.47   | 9.33   | 9.650  | 10.20  | 10.10  | 10.26  | 10.10  | 9.69   | 10.22        | 10.22  | 9.28   | 9.27   | 9.27   | 9.55   | 9.91   | 9.77   |
| K <sub>2</sub> O                 | -          | -      | -      | -      | 0.13   | -      | -      | -      | -      | 0.10   | 0.10   | -            | 0.10   | 0.16   | 0.28   | 0.07   | 0.60   | 0.22   | 0.16   |
| Total                            | 99.69      | 100.68 | 100.30 | 100.50 | 99.47  | 99.89  | 100.04 | 99.71  | 99.94  | 99.78  | 100.14 | 99.98        | 99.60  | 100.67 | 99.65  | 99.79  | 100.01 | 99.81  | 99.03  |
| Si <i>apfu</i>                   | 3.983      | 3.997  | 4.000  | 4.048  | 4.035  | 3.99   | 4.035  | 3.998  | 4.001  | 3.991  | 4.045  | 4.049        | 4.050  | 3.963  | 3.955  | 3.991  | 4.016  | 4.059  | 4.007  |
| Al                               | 4.025      | 4.012  | 3.957  | 3.946  | 3.974  | 4.032  | 3.999  | 4.040  | 4.039  | 4.060  | 4.003  | 4.005        | 3.973  | 4.030  | 4.055  | 4.017  | 3.974  | 3.924  | 4.034  |
| Fe                               | -          | -      | 0.028  | -      | -      | -      | -      | -      | -      | -      | 0.020  | -            | 0.024  | 0.029  | 0.053  | 0.028  | 0.019  | 0.100  | 0.027  |
| Si:Al                            | 0.989      | 0.996  | 1.011  | 1.026  | 1.015  | 0.990  | 1.009  | 0.990  | 0.991  | 0.983  | 1.011  | 1.011        | 1.019  | 0.983  | 0.975  | 0.994  | 1.010  | 1.034  | 0.993  |
| Ca                               | -          | -      | -      | -      | -      | -      | 0.007  | -      | -      | -      | -      | -            | -      | 0.012  | 0.000  | 0.008  | 0.023  | 0.006  | 0.000  |
| Sr                               | 0.271      | 0.377  | 0.041  | 0.194  | 0.258  | 0.337  | 0.407  | 0.564  | 0.635  | 0.791  | 0.847  | 0.883        | 0.850  | 0.067  | 0.215  | 0.506  | 0.696  | 0.791  | 0.874  |
| Ba                               | 0.729      | 0.570  | 0.978  | 0.804  | 0.726  | 0.638  | 0.487  | 0.361  | 0.281  | 0.132  | 0.074  | 0.017        | 0.045  | 0.919  | 0.727  | 0.482  | 0.261  | 0.063  | 0.044  |
| ΣA                               | 1.000      | 0.947  | 1.019  | 0.998  | 0.984  | 0.975  | 0.901  | 0.925  | 0.916  | 0.923  | 0.921  | 0.900        | 0.895  | 0.998  | 0.942  | 0.996  | 0.980  | 0.860  | 0.918  |
| Sr:Ba                            | 0.372      | 0.662  | 0.042  | 0.242  | 0.356  | 0.528  | 0.835  | 1.562  | 2.260  | 5.996  | 11.459 | 53.415       | 18.976 | 0.073  | 0.295  | 1.050  | 2.663  | 12.583 | 19.704 |
| Na                               | 1.995      | 2.084  | 2.006  | 1.973  | 1.951  | 1.995  | 2.064  | 2.037  | 2.050  | 1.997  | 1.896  | 1.989        | 2.005  | 1.951  | 1.933  | 1.897  | 1.917  | 1.940  | 1.932  |
| K                                | -          | -      | -      | -      | 0.018  | -      | -      | -      | -      | 0.013  | 0.013  | -            | 0.013  | 0.022  | 0.038  | 0.009  | 0.079  | 0.028  | 0.021  |
| Σcat                             | 11.003     | 11.040 | 11.011 | 10.966 | 10.962 | 10.990 | 10.998 | 11.000 | 11.005 | 10.984 | 10.898 | 10.943       | 10.960 | 10.994 | 10.976 | 10.939 | 10.985 | 10.913 | 10.939 |

\* total iron is given as Fe<sub>2</sub>O<sub>3</sub>; - not detected. Compositions are reported in wt.%, then recast in terms of atoms per formula unit (*apfu*). 1–13: Pilansberg peralkaline complex: 1, 2 in white foyaite, 3–12 in lujavrite, 13 in "Ledig" foyaite. Columns 14–19: Prairie Lake complex. The structural formulae calculated on the basis of 16 atoms of oxygen.

site–stronalsite series was formed as a by-product of the nepheline-to-analcime conversion, and did not crystallize in a paragenesis with sodalite replacing nepheline at a high-temperature postmagmatic stage.

In lujavrite, stronalsite formed contemporaneously with other Sr-rich minerals. The crystallization of closely associated strontium-apatite, lamprophyllite and stronalsite indicates high activities of Sr, which might result from the decomposition of a Sr-rich member of the eudialyte group (4.5–8 wt.% SrO), which is abundant in the lujavrite (Mitchell & Liferovich 2005). Similar Sr-rich eudialyte is common in the white foyaite. Stronalsite is also associated with the Mn-rich minerals, kupletskite and zincian pyrophanite (Mitchell & Liferovich 2004), indicating that the fluid responsible for the crystallization of the banalsite–stronalsite<sub>ss</sub> was also enriched in Mn<sup>2+</sup>, and thus similar to the alkaline

fluids that deposited banalsite at the Benallt mine and Långban, and stronalsite at Khibina.

The complete banalsite–stronalsite series is developed in lujavrite (Table 4, comp. 3–12, Fig. 2). In white foyaite, where Sr-rich eudialyte is not abundant, the series does not reach the end-member composition of stronalsite (Table 4, comp. 1, 2). In the strontium-rich Ledig foyaite (Lurie 1986), only stronalsite is observed (Table 4, comp. 13; Fig. 4d). The latter might represent complete pseudomorphs after former banalsite, similar to those observed in lujavrite and white foyaite. Calcium, K, and Fe are absent or present only in very low amounts in the banalsite–stronalsite series (Table 4, comp. 1–13). The banalsite–stronalsite<sub>ss</sub> aggregates were subjected to epigenetic alteration following the replacement of analcime by natrolite and unidentified Na–Ca zeolite(s).

*The Prairie Lake alkaline complex, Ontario, Canada*

Various tectosilicates of barium and strontium are common in alkaline silicate rocks of the Prairie Lake complex. Postmagmatic processes affected all rock units in this multistage ring-complex (Sage 1987). The late-magmatic and postmagmatic parageneses in diverse ijolite units, phlogopite glimmerite, and alkaline pyroxenite contain hyalophane,  $\text{BaAl}_2\text{Si}_2\text{O}_8$  (celsian, paracelsian, or both), slawsonite, banalsite, stronalsite and a near-complete solid-solution series between the latter two minerals.

Compositionally homogeneous grains of stronalsite are observed in strongly altered and mechanically stressed xenoliths grading from apatite–calcite-bearing stronalsite clinopyroxenite to serpentine–calcite mylonite. These ultramafic alkaline xenoliths are hosted by veins of massive medium-grained wollastonite ijolite. Stronalsite occurs as subhedral grains 0.2–0.5 mm in diameter, and is a complete pseudomorph after primary nepheline, as deduced from its stubby prismatic habit and the presence of rare nepheline relics in the stronalsite aggregates (Fig. 1d). These grains are poiki-

litically enclosed by grains of clinopyroxene that grade from primary diopside in the core to aegirine–diopside at the rim. Stronalsite grains contain numerous small inclusions of analcime together with slawsonite, fluorapatite, and calcite. In a few cases, minute relics of strongly altered nepheline (“hydronepheline”?) are observed in grains of slawsonite and stronalsite. In addition, small grains of stronalsite ( $\leq 15 \mu\text{m}$ ) are present together with slawsonite in analcime pseudomorphs after nepheline in xenoliths of phlogopite glimmerite. These xenoliths are hosted by a late dyke of porphyroclastic magnetite-rich calciocarbonatite. Stronalsite is coeval with analcime, tetra-ferriphlogopite and Al-poor aegirine–diopside replacing nepheline, phlogopite and diopside, respectively. This stronalsite contains considerable amounts of Fe and low to undetectable quantities of Ca and K (Table 2, comp. 7, 8).

In addition to stronalsite in the xenoliths, the banalsite–stronalsite<sub>ss</sub> series is found in diverse rocks of the ijolite series, including coarse-grained wollastonite and garnet-rich ijolite, which commonly grade to medium- and fine-grained melteigite. Unaltered rocks with fresh nepheline do not contain banalsite–stronalsite<sub>ss</sub>, and the

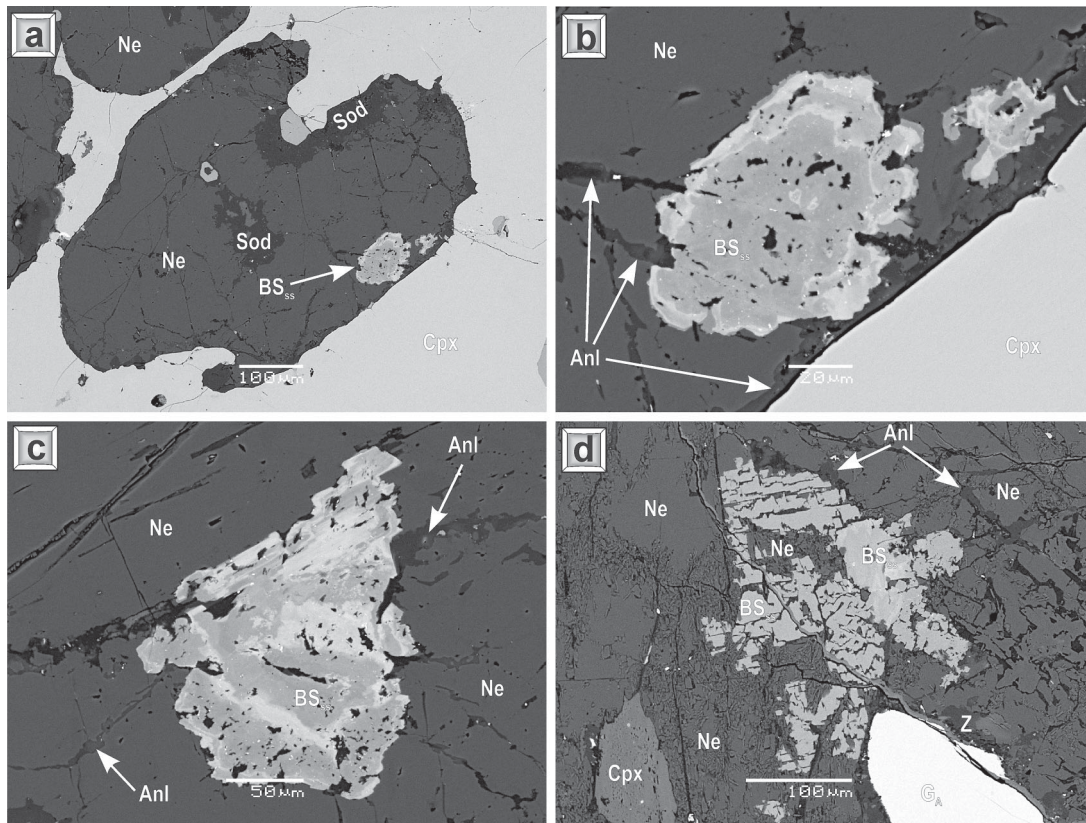


FIG. 5. Back-scattered-electron images showing textural features of the banalsite–stronalsite solid-solution series in ijolite from the Prairie Lake ultramafic–alkaline complex, northwestern Ontario, Canada.

series appears only in feldspathoidal rocks subjected to postmagmatic alteration. As a rule, alteration affected the rocks in the vicinity of contacts with rocks of the younger carbonatite series, or around xenoliths of alkaline pyroxenite and glimmerite. The modal composition of the altered feldspathoidal rocks is highly variable, as several generations of major and accessory phases are present. Accessories include early wollastonite, zircon, Zr–Ti-rich garnet, and a variety of pyrochlore-group minerals, followed by late-stage pectolite, loparite-(Ce) and marianite (the Nb-analog of wöhlerite, IMA 2005–05a). Commonly, poikilitic subhedral aggregates of banalsite–stronalsite<sub>ss</sub> are confined to the periphery of nepheline crystals (Fig. 5a), or to analcime-filled cracks cutting these crystals (Figs. 5b, c, d). The aggregates typically entrap small inclusions of analcime. Banalsite–stronalsite<sub>ss</sub> is not associated with sodalite (Fig. 5a). In some instances, stronalsite forms botryoidal aggregates of co-oriented micrograins within nepheline (Fig. 5d), suggesting a possible epitaxial relationship. Typically, banalsite forms a high-AZ core (Fig. 5c) and, in some cases, appears as concentric zones within barian stronalsite (Figs. 5b, c). The character of the zoning implies that crystallization of the tectosilicates began at high  $a_{Ba}$  and continued with oscillations of  $a_{Ba}$  and  $a_{Sr}$ . Members of the essentially complete  $Ba_{1-x}Sr_xNa_2Al_4Si_4O_{16}$  solid solution observed in the Prairie Lake samples (Fig. 2) have low but detectable amounts of Ca, K and Fe (Table 4, comp. 14–19). In a single example, stronalsite with 0.87 *apfu* (Sr + Ba + Ca) contains 1.3 wt.%  $Fe_2O_3$  (0.10 *apfu*  $Fe^{3+}$ ), probably compensating for the <sup>X</sup>A-site deficiency (Table 4, comp. 18).

#### DISCUSSION AND CONCLUSIONS

Banalsite and stronalsite, including compositional intermediates of the series, contain only very limited amounts of alkalis and alkaline-earth cations other than Na, Ba, and Sr. This empirical observation accords well with the structural difference between banalsite–stronalsite and other alkali and alkaline-earth tectosilicates. Our data show that where present, Ca and K show no conspicuous correlation with any deficiency at the <sup>X</sup>A and <sup>V1</sup>Na sites in the banalsite–stronalsite<sub>ss</sub>.

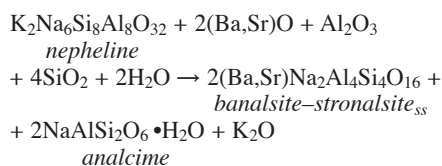
Regarding the origin of the Ba–Sr tectosilicates, our compositional and paragenetic data indicate that they can form by three processes. One is direct crystallization of banalsite from a silica-undersaturated sodic magma. Inclusions of banalsite grains along concentric zones in nepheline crystals in lujavrite at Pilansberg and at the margins of nepheline crystals in ijolite at Prairie Lake suggest that banalsite might crystallize at a late-magmatic stage, together with nepheline.

Banalsite has formed in the metamorphic sequence at the Benallt mine and in glimmerite at Långban. Stronalsite has formed in high-grade metamorphic rocks and altered ultramafic xenoliths (Matsubara 1985, Hori *et al.* 1987, Khomyakov *et al.* 1990), suggesting that

metamorphic (metasomatic) alkaline fluids are capable of depositing these Na–Ba(Sr) tectosilicates.

The most common mode of formation of banalsite–stronalsite<sub>ss</sub> is inferred from the consistent textural relationships between primary nepheline and a secondary assemblage consisting of analcime (the major phase) and banalsite–stronalsite<sub>ss</sub> (commonly, the minor phase; Figs. 3a, c, 4a, b, d, 5c, d). The textures imply that banalsite–stronalsite<sub>ss</sub> forms at a late stage by subsolidus reaction of primary nepheline with a deuteric alkaline fluid.

Schematically, the replacement might be expressed as:



This mechanism of alteration of nepheline increases alkalinity (agpaicity) of the mineral-forming fluid system by release of K and removal of Al and Si. The K released during this reaction is precipitated as late K-rich feldspar, leucite, biotite, kupletskite, and other minerals associated with banalsite–stronalsite<sub>ss</sub>.

The formation of banalsite and stronalsite at the expense of nepheline is facilitated by the gross structural similarities between these tectosilicates: (i) Their structures are based on an ordered infinite framework with a Si-to-Al ratio of unity (Tait *et al.* 2003, Liferovich *et al.* 2006), (ii) in both structures, vertex-connected tetrahedra form –UDUD– rings connected into sheets parallel to (001) in banalsite–stronalsite, and (0001) in nepheline (Tait *et al.* 2003), and (iii) in both structures, large cations occupy cages within the frameworks and are affected by subsolidus leaching and cation exchange with deuteric fluid.

Replacement of *P6*<sub>3</sub>-structured nepheline by *Iba*<sub>2</sub>-structured banalsite–stronalsite<sub>ss</sub> results from deuteric leaching of <sup>138</sup>K<sup>+</sup> cations and their replacement by <sup>X</sup>(Ba,Sr)<sup>2+</sup> cations. This results in a re-arrangement of the nepheline framework of regular and irregular six-member rings (Tait *et al.* 2003) to the banalsite–stronalsite framework, based on irregular four- and eight-member rings (Liferovich *et al.* 2006).

The crystallization of the banalsite–stronalsite<sub>ss</sub> series at the expense of nepheline is a characteristic feature of specific physical–chemical conditions existing during the deuteric alteration of the feldspathoidal rocks. These conditions are responsible for the crystallization of late analcime or albite after nepheline. As residual nepheline mantled by the banalsite–stronalsite<sub>ss</sub> aggregates has a stoichiometric or near-stoichiometric composition within the Morozewicz–Burger convergence field, the temperature of banalsite–stronalsite crystallization must have been less than 500°C (Hamilton 1961). Marks &

Markl (2003) have developed a quantitative model for nepheline-to-analcime conversion during the autometamorphic alteration of sodic peralkaline rocks. According to this model, nepheline is replaced by analcime at temperatures below 300°C, H<sub>2</sub>O activities of between 0.5 and unity, and oxygen fugacities above the magnetite-hematite buffer. These conditions are applicable to the crystallization of the banalsite-stronalsite<sub>ss</sub> as a replacement of nepheline coeval with analcime. The appearance of abundant Ba-Sr tectosilicates replacing nepheline in the subvolcanic nepheline syenite series at the Pilansberg complex indicates a low-pressure genesis (probably, below 0.1 GPa).

Textural relationships show that banalsite-stronalsite<sub>ss</sub> either does not form during the stage of postmagmatic conversion of nepheline to sodalite or cancrinite, or it has not been preserved. This observation implies that banalsite-stronalsite<sub>ss</sub> is not stable at elevated concentrations of chlorine or sulfur in the fluid, or does not form at the *P-T* conditions suitable for crystallization of sodalite or cancrinite. Being formed at a late-magmatic or an early postmagmatic stage, these tectosilicates of Na, Ba and Sr are not stable at the low-temperature deuteric stage, and can be subject to alteration contemporaneously with the formation of natrolite and Na-Ca zeolite(s) at the expense of nepheline and analcime. Our study of weathered nepheline syenite from various complexes (including Coldwell, Khibina, Lovozero, Prairie Lake, Salmagorskiy, Sebljavr, Sokli, Vuorijarvi) shows that epigenetic alteration of nepheline results in replacement by so-called "liebenerite" and "spreusteine" (greyish green and brownish red white mica - zeolite - oxide secondary aggregates, respectively) and does not form Ba-Sr tectosilicates.

Banalsite, stronalsite and their complete solid-solution series are expected to be common postmagmatic phases in fluid-rich nepheline syenite and alkaline ultramafic rocks subject to postmagmatic alteration. We should note that banalsite-stronalsite<sub>ss</sub> commonly occurs as optically irresolvable tiny inclusions in nepheline. Thus, bulk compositional data on the content of Sr and Ba in nepheline should be regarded with caution.

The reaction producing stronalsite at the expense of nepheline in natural deuteric alkaline systems consanguineous with nepheline-rich alkaline rocks could be employed for safe disposal of <sup>90</sup>Sr fission products from fuel-reprocessing nuclear waste. In contrast to the technology employed currently for processing such <sup>90</sup>Sr-bearing wastes, a new technology might permit the avoidance of techniques using fluorine at high temperatures, and would utilize nepheline, a low-cost mineral commodity.

#### ACKNOWLEDGEMENTS

This work is supported by the Natural Sciences and Engineering Research Council of Canada and Lakehead University (Canada). We thank Allan MacKenzie for

assistance with analytical work, and Anne Hammond for sample preparation. Dr. R.C. (Jock) Harmer is thanked for assistance with collection of Pilansberg syenites. The Director of the Pilansberg National Park is thanked for permission to undertake geological investigations in the Park area. The authors are grateful to Satoshi Matsubara (Science Museum, Tokyo), Knut Eldjarn (Norway), Nick Woodhouse (UK), and Tony Nikischer (Excalibur Mineral Corp., USA) for providing stronalsite and banalsite samples. The comments and suggestions of two anonymous reviewers and Robert F. Martin helped to improve the initial version of this manuscript. Editorial care and help from Dana T. Griffen and Robert F. Martin are highly appreciated.

#### REFERENCES

- ARZAMASTSEV, A.A., BEA, F., ARZAMASTSEVA, L.V., MONTERO, P. & VINOGRADOV, A.N. (2003): Multistage alkaline massif of Greymykh-Vyrmes, Kola peninsula: U-Pb, Rb-Sr and Sm-Nd dating of the intrusive series and estimation of their sources composition. *In* *Geochemistry of Magmatic Rocks* (A.A. Arzamastsev, ed.). Kola Science Centre, Russian Academy of Sciences, Apatity, Russia (19-20, in Russ.).
- BATIEVA, I.D. & BELKOV, I.V. (1984): *Sakharjok Alkaline Massif and its Petrological and Mineralogical Features*. Kola Science Centre, Russian Academy of Sciences, Apatity, Russia (in Russ.).
- BELL, K., DUNWORTH, E.A., BULAKH A.G. & IVANIKOV, V.V. (1996): Alkaline rocks of the Turij Massif, Kola Peninsula, including type-locality turjaite and turjite: a review. *Can. Mineral.* **34**, 265-280.
- CAMPBELL SMITH, W. (1944): Banalsite crystals from Wales. *Mineral. Mag.* **27**, 63-64.
- CAMPBELL SMITH, W., BANNISTER, F.A. & HEY, M.H. (1944a): A new barium-feldspar from Wales. *Nature* **154**, 336-337.
- CAMPBELL SMITH, W., BANNISTER, F.A. & HEY, M.H. (1944b): Banalsite, a new barium-feldspar from Wales. *Mineral. Mag.* **27**, 33-47.
- CHAKHMOURADIAN, A.R. & MITCHELL, R.H. (1999): Primary, apatitic and deuteric stages in the evolution of accessory Sr, REE, Ba and Nb-mineralization in nepheline-syenite pegmatites at Pegmatite Peak, Bearpaw Mts., Montana. *Mineral. Petrol.* **67**, 85-110.
- CHAKHMOURADIAN, A.R. & MITCHELL, R.H. (2002): The mineralogy of Ba- and Zr-rich pegmatites from Gordon Butte, Crazy Mountains (Montana, USA): comparisons between potassic and sodic apatitic pegmatites. *Contrib. Mineral. Petrol.* **143**, 93-114.
- DEER, W.A., HOWIE, R.A. & ZUSSMAN, J. (2001): *Rock-Forming Minerals. 4A. Framework Silicates: Feldspars*. Geological Society, London, U.K.

- DUNWORTH, E.A. & BELL, K. (2003): The Turij massif, Kola peninsula, Russia: mineral chemistry of an ultramafic-alkaline – carbonatite intrusion. *Mineral. Mag.* **67**, 423-451.
- FERGUSON, J. (1973): The Pilansberg alkaline province. *Trans. Geol. Soc. S. Africa* **76**, 207-214.
- HAMILTON, D.L. (1961): Nepheline as crystallization temperature indicators. *J. Geol.* **69**, 321-329.
- HARLOW, G.E. & OLDS, E.P. (1987): Observations on terrestrial ureyite and ureyitic pyroxene. *Am. Mineral.* **72**, 126-136.
- HORI, H., NAKAI, I., NAGASHIMA, K., MATSUBARA S. & KATO, A. (1987): Stronalsite,  $\text{SrNa}_2\text{Al}_4\text{Si}_4\text{O}_{16}$ , a new mineral from Rendai, Kochi City, Japan. *Mineral. J.* **13**, 368-375.
- KHOMYAKOV, A.P. (1995): *Mineralogy of Hyperagpaitic Alkaline Rocks*. Clarendon Press, Oxford, U.K.
- KHOMYAKOV, A.P., SHPACHENKO, A.K. & POLEZHAIEVA, L.I. (1990): Melilite and rare earth phosphate mineralization at the Namuaiv Mount (Khibina). In *Alkaline Magmatism at the NE part of the Baltic Shield* (T.N. Ivanova, O.B. Dudkin & A.A. Arzamastsev, eds.). Kola Science Centre, Russian Academy of Sciences, Apatity, Russia (106-119).
- KONEVA, M.A. (1996): Banalsite and stronalsite from pyroxenites of the Zhidoy massif (the first Russian occurrence). *Zap. Vser. Mineral. Obschest.* **152**(2), 103-108 (in Russ.).
- KUKHARENKO, A.A., ORLOVA, M.P., BULAKH, A.G., BAGDASAROV, E.A., RIMSKAYA-KORSAKOVA, O.M., NEFEDOV, E.I., IL'INSKIY, G.A., SERGEEV, A.S. & ABAKUMOVA, N.B. (1965): *The Caledonian Ultramafic Alkaline and Carbonatite Complexes of the Kola Peninsula and Northern Karelia*. Nedra, Moscow, USSR (in Russ.).
- LIFEROVICH, R.P., MITCHELL, R.H., LOCOCK, A. & SPACHENKO, A.K. (2006): Crystal structure of stronalsite and a re-determination of the crystal structure of banalsite. *Can. Mineral.* **44**, 533-546.
- LOEWENSTEIN, W. (1954): The distribution of aluminum in the tetrahedra of silicates and aluminates. *Am. Mineral.* **39**, 92-96.
- LURIE, J. (1973): *The Pilansberg: Geology, Rare Element Geochemistry and Economic Potential*. Ph.D. thesis, Rhodes Univ., Grahamstown, South Africa.
- LURIE, J. (1986): Mineralization of the Pilansberg alkaline complex. In *Mineral Deposits of Southern Africa 2* (C.R. Anhaeusser & S. Maske, eds.). Geological Society of South Africa, Johannesburg, South Africa (2215-2228).
- MARKL, G., MARKS, M., SCHWINN, G. & SOMMER, H. (2001): Phase equilibrium constraints on intensive crystallization parameters of the Ilímaussaq complex, South Greenland. *J. Petrol.* **42**, 2231-2258.
- MARKS, M. & MARKL, G. (2003): Ilímaussaq “en miniature”: closed-system fractionation in an agpaitic dyke rock from the Gardar Province, South Greenland. *Mineral. Mag.* **67**, 893-919.
- MATSUBARA, S. (1985): The mineralogical implication of barium and strontium silicates. *Bull. Nat. Sci. Mus. (Tokyo)* **11C**, 37-95.
- MITCHELL, R.H. & LIFEROVICH, R.P. (2004): Ecanndrewsite – zincian pyrophanite from lujavrite, Pilansberg alkaline complex, South Africa. *Can. Mineral.* **42**, 1169-1178.
- MITCHELL, R.H. & LIFEROVICH, R.P. (2005): Subsolidus deuteric/hydrothermal alteration of eudialyte in aegirine lujavrite, Pilansberg alkaline complex, South Africa. In *Peralkaline Rocks: Sources, Economic Potential and Evolution from Alkaline Melts* (M. Marks, ed). PERALK Workshop (Tübingen), Abstr. Vol., 74-76.
- MITCHELL R.H. & VLADYKIN, N.V. (1993): Rare earth elements-bearing tausonite and potassium barium titanates from the Little Murun potassic alkaline complex, Yakutia, Russia. *Mineral. Mag.* **57**, 651-664.
- OLIVO, G.R. & WILLIAMS-JONES, A.E. (1999): Hydrothermal REE-rich eudialyte from the Pilansberg complex, South Africa. *Can. Mineral.* **37**, 653-663.
- RETIEF, E.A. (1962): Preliminary observations on the feldspars from the Pilansberg alkaline complex, Transvaal, S. Africa. *Norsk Geol. Tidsskr.* **42**, 493-513.
- RETIEF, E.A. (1963): *Petrological and Mineralogical Studies in the Southern Part of the Pilansberg Complex, Transvaal, South Africa*. Ph.D. thesis, Univ. of Oxford, Oxford, U.K.
- ROSSI, G., OBERTI, R. & SMITH, D.C. (1986): Crystal structure of lisetite,  $\text{CaNa}_2\text{Al}_4\text{Si}_4\text{O}_{16}$ . *Am. Mineral.* **71**, 1378-1383.
- SAGE, R.P. (1987): Geology of carbonatite – alkalic rock complexes in Ontario: Prairie Lake carbonatite complex, district of Thunder Bay. *Ministry of Northern Development and Mines, Ontario Geol. Surv.* **46**.
- SHAND, S.I. (1928): The geology of Pilansberg in the Western Transvaal. *Trans. Geol. Soc. S. Afr.* **31**, 91-156.
- TAIT, K.T., SOKOLOVA, E., HAWTHORNE, F.C. & KHOMYAKOV, A.P. (2003): The crystal chemistry of nepheline. *Can. Mineral.* **41**, 61-70.
- WELIN, E. (1968): X-ray powder diffraction data for minerals from Långban and related mineral deposits of central Sweden. *Arkiv Mineral. Geol.* **4**, 499-541.
- WILKINSON, J.F.G. & HENSEL, H.D. (1994): Nephelines and analcimes in some alkaline igneous rocks. *Contrib. Mineral. Petrol.* **118**, 79-91.
- ZOZYLYA, D.R., EBY, G.N. & BAYANOVA, T.B. (2001): Keivy alkaline magmatism in the NE Baltic Shield: evidence for the presence of an enriched reservoir in Late Archaean mantle. *Fourth International Archaean Symp., Extended Abstr.* **37**, 540-542.

Received April 28, 2005, revised manuscript accepted December 27, 2005.